ANTIOXIDANTS & REDOX SIGNALING
Volume 14, Number 1, 2011

DOI: 10.1089/ars.2010.3095

ORIGINAL RESEARCH COMMUNICATION

Role of Apoptosis Signal-Regulating Kinase-1-c-Jun NH_2-Terminal Kinase-p38 Signaling in Voltage-Gated K^+ Channel Remodeling of the Failing Heart: Regulation by Thioredoxin

Kang Tang,[1] Xun Li,[2] Ming-Qi Zheng,[1,3] and George J. Rozanski[1,4]

Abstract

c-Jun NH_2-terminal kinase (JNK) and p38 kinase are key regulators of cardiac hypertrophy and apoptosis during pathological stress, but their role in regulating ion channels in the diseased heart is unclear. Thus, we compared the kinase profile and electrophysiological phenotype of the rat ventricle 6–8 weeks after myocardial infarction (MI). Molecular analyses showed that JNK and p38 activities were markedly increased in post-MI hearts, while parallel voltage-clamp studies in ventricular myocytes revealed a characteristic downregulation of transient outward K^+ current (I_{to}) density. When post-MI myocytes were treated with JNK or p38 inhibitors, I_{to} density increased to control levels. Upregulation of I_{to} was also elicited by insulin-like growth factor-1, which decreased JNK/p38 activity in post-MI hearts, and these changes were blocked by the thioredoxin (Trx) reductase inhibitor auranofin. Consistent with activation of JNK-p38 signaling, binding of apoptosis signal-regulating kinase-1 with Trx1 was also markedly decreased post-MI, and was reversed by insulin-like growth factor-1 in an auranofin-sensitive manner. We conclude that expression of ventricular K^+ channels is redox regulated and that chronic impairment of the Trx system in the post-MI heart contributes to I_{to} remodeling through sustained activation of apoptosis signal-regulating kinase-1-JNK-p38 signaling. The cardiac Trx system may thus be a novel therapeutic target to reverse or prevent ventricular arrhythmias in the failing heart. *Antioxid. Redox Signal.* 14, 25–35.

Introduction

The failing heart undergoes a pathogenic process of electrical remodeling that is postulated to contribute to ventricular contractile dysfunction and increased risk of lethal arrhythmias in heart failure patients (2). Although the electrophysiology of the remodeled ventricle involves changes in several types of ion channels, downregulation of voltage-gated K^+ (Kv) channels underlying the transient outward K^+ current (I_{to}) is perhaps the most consistent change observed in heart failure, both in the human heart (2, 14) and in animal models (2, 15, 20, 22, 33). In rodent hearts, a disease-related decrease in Kv channel expression participates in prolongation of the ventricular muscle action potential and alterations in refractory period (15). However, while prolonged action potential duration is also a hallmark of the electrically remodeled human ventricle, experiments in larger mammals suggest that I_{to} downregulation contributes more to the dysfunction of Ca^{2+}_i regulation and contraction than to prolongation of the action potential (8). Nevertheless, our understanding of the cellular mechanisms underlying downregulation of Kv channel expression and I_{to} density in the failing heart is incomplete.

Recent experimental studies have identified oxidative stress as a key contributor to cardiac ion channel remodeling, particularly Kv4 channels (20, 22, 33). Moreover, our laboratory has shown that endogenous oxidoreductase networks are capable of reversing channel remodeling, a process termed de-remodeling (20, 22, 33). In particular, we have reported that the characteristic decrease in Kv channel expression and I_{to} density in ventricular myocytes from rats with chronic myocardial infarction (MI) can be reversed *in vitro* by exogenous stimuli that increase the activity of the ubiquitous thioredoxin (Trx) system (20, 22). In the cytoplasm of mammalian cells, this endogenous redox network is composed of Trx1, Trx reductase-1 (TrxR1), and glucose-derived NADPH

[1]Department of Cellular and Integrative Physiology, University of Nebraska Medical Center, Omaha, Nebraska.
[2]Department of Cardiology, The First Affiliated Hospital, Suzhou University, Jiangsu, P.R. China.
[3]Heart Center, The First Hospital of Hebei Medical University, Shijiazhuang, P.R. China.
[4]Redox Biological Center, University of Nebraska-Lincoln, Lincoln, Nebraska.

(30, 35, 45). The functionally related glutaredoxin (Grx) system also contributes to overall oxidoreductase activity (5), but its role in regulating Kv channel expression is less understood. Nevertheless, these oxidoreductase systems importantly function as cellular repair networks protecting proteins from oxidative damage (5, 30, 35), but the underlying molecular mechanisms by which they regulate the electrophysiological phenotype of the heart are not well defined. Thus, the objective of the present study was to identify targets of the Trx system that mediate Kv channel remodeling in the rat heart with chronic MI. Our data identify apoptosis signal-regulating kinase-1 (ASK1) as a key binding partner for Trx1 that controls Kv current density in the post-MI rat heart and suggest that decreased ASK1–Trx1 interaction mediates Kv channel downregulation *via* sustained activation of the downstream effectors, c-Jun NH_2-terminal kinase (JNK) and p38 kinase. Thus, we propose that the Trx system may be a therapeutic target to reverse or prevent pathogenic electrical remodeling in the failing heart, thereby improving contractile function and decreasing arrhythmogenesis.

Materials and Methods

Rat post-MI model

All animal procedures were carried out in accordance with guidelines approved by the University of Nebraska Medical Center Institutional Animal Care and Use Committee, and conducted according to the *Guide for the Care and Use of Laboratory Animals* published by the U.S. National Institutes of Health (NIH Publication No. 85-23, revised 1996).

A chronic MI model of ventricular dysfunction was used in the present investigation as described previously (22, 33, 42). Briefly, male Sprague–Dawley rats (180–200 g) were intubated and artificially ventilated under Brevital (methohexital® sodium) anesthesia at 50 mg/kg, i.p. A left thoracotomy was performed and the left coronary artery was ligated by a suture positioned between the pulmonary artery outflow tract and the left atrium. This ligation procedure typically produced infarcts of 30%–40% of the left ventricular free wall and physiological signs of heart failure after several weeks (42). Sham-operated animals that served as controls underwent the same surgical procedure but were not subjected to coronary artery ligation.

The post-MI model of chronic ventricular dysfunction used in these studies is characterized by echocardiographic alterations similar to those observed clinically in patients with heart failure, including a 35% decrease in left ventricular ejection fraction, 45% decrease in fractional shortening, and a 45% increase in left ventricular end diastolic volume (42). In addition, there is compensatory hypertrophy of the surviving myocardium as reflected by a marked increase in heart weight-to-body weight ratio (33, 42). At the cellular level, this model is characterized by marked alterations in redox balance, particularly increased superoxide production, reduced glutathione (GSH) depletion, and significant decreases in the activities of γ-glutamylcysteine synthetase, glutathione reductase, and TrxR1, compared with sham-operated control rats (22, 33). Thus, the chronic dysfunction of the left ventricle elicited by MI is paralleled by markers of oxidative stress and resulting shift in cell redox state.

Six to 8 weeks after MI or sham operation, rats were given an overdose of pentobarbital sodium (100 mg/kg, i.p.) and the hearts were excised and perfused *via* the coronary vasculature by the Langendorff method. In some experiments, myocytes were dissociated from perfused hearts by a collagenase digestion procedure described previously (20, 22, 33). Dispersed myocytes from surviving regions of the left ventricle and septum were suspended in Dulbecco's modified Eagle's medium/Ham's F12 (DMEM/F12) and stored in an incubator at 37°C until used, usually within 6 h of isolation. In a second group of experiments, isolated hearts were perfused for 4–5 h at a constant pressure of 100 cm of water with oxygenated DMEM/F12 maintained at 37°C and containing 3% Dextran. Blebbistatin (5 μM) was also added to the perfusate to block contraction (4). After the perfusion period, samples of left ventricle and septum were dissected and rapidly frozen for subsequent molecular and biochemical analyses. Unless stated otherwise, all reagents were purchased from Sigma-Aldrich Chemical (St. Louis, MO).

Western blotting

Samples of left ventricle or septum were homogenized in ice-cold Tris-ethylenediaminetetraacetic acid (TE) buffer (10 m*M* Tris-HCl, 1 m*M* EDTA, pH 7.4) containing a protease inhibitor cocktail. The homogenates were centrifuged at 1000 *g* for 10 min to remove nuclei and debris, and the pellets were re-suspended in TE buffer, homogenized, and centrifuged again. The supernatants from both low-speed spins were pooled and centrifuged at 40,000 *g* for 15 min. The resulting pellets were re-suspended in TE buffer containing 600 m*M* potassium iodide to dissociate myofibrillar proteins. After centrifugation at 40,000 *g* for an additional 10 min, the pellets were washed twice with TE buffer and solubilized in TE buffer containing 2% Triton X-100 on ice for 1 h. Insoluble material was centrifuged at 15,000 *g* for 15 min.

Equal amounts of proteins from each sample were separated by sodium dodecyl sulfate-polyacrylamide gel electrophoresis (SDS-PAGE) and transferred to polyvinylidene difluoride membrane. Blots were blocked by a commercial buffer (Pierce, Rockford, IL) with 5% dry milk for 1 h at room temperature. Anti-phospho-JNK, anti-JNK, anti-phospho-p38, and anti-p38 (Cell Signaling Technology, Beverly, MA) were used to assess JNK and p38 activation, while protein abundance of TrxR1, glyceraldehyde 3-phosphate dehydrogenase, and Kv4.2 were determined using anti-TrxR1, anti-glyceraldehyde 3-phosphate dehydrogenase (Santa Cruz Biotechnology, Santa Cruz, CA), and anti-Kv4.2 (Alamone Labs, Tel Aviv, Israel), respectively. Signals were observed using ECL advanced Western blotting detection kit (GE Healthcare, Piscataway, NJ), digitized with a UVP BioImaging System (Upland, CA), and quantified with Multi Gauge software (FujiFilm, Valhalla, NY).

JNK and p38 activity assay

Activation of JNK was assessed by two methods. The first was by immunoblotting with a phosphospecific antibody (Cell Signaling Technology) and the second was by a nonradioactive JNK kinase assay kit (Cell Signaling Technology) according to the manufacturer's instructions. In the latter, tissue homogenates were first prepared with lysis buffer (Tris 20 m*M*, pH 7.4, NaCl 150 m*M*, EDTA 1 m*M*, ethylene glycol-bis(2-aminoethyl-ether)-*N*,*N*,*N*′,*N*′-tetraacetic acid (EGTA) 1 m*M*, Triton 1%, sodium pyrophosphate 2.5 m*M*, glycer-

olphosphate 1 m*M*, sodium orthovanadate 1 m*M*, and leupeptin 1 μg/ml). After centrifugation at 15,000 *g* for 30 min at 4°C, the supernatant was saved and protein concentration was measured by bicinchoninic acid (BCA) protein assay. Proteins (0.4 mg) were incubated with 20 μl of an immobilized c-Jun fusion protein bead slurry overnight at 4°C. The immunoprecipitates were washed twice with lysis buffer and twice with kinase buffer (Tris 25 m*M*, pH 7.4, glycerolphosphate 5 m*M*, DL-dithio-threitol (DTT) 2 m*M*, $MgCl_2$ 10 m*M*, and sodium orthovanadate 0.1 m*M*). The pellets were suspended in 50 μl of kinase buffer supplemented with 0.2 m*M* ATP for 30 min at 30°C. After incubation the kinase reaction was stopped by the addition of a 4×Laemmli sample buffer. Ten microliters of the supernatant was subjected to SDS-PAGE and the bands of phosphorylated c-Jun fusion protein were detected by a phospho-c-Jun (Ser63) antibody.

Activation of p38 kinase was assessed by a nonradioactive p38 kinase assay kit (Cell Signaling Technology) according to the manufacturer's instructions. Briefly, homogenates from tissue samples were prepared with lysis buffer as above. After centrifugation at 15,000 *g* for 30 min at 4°C, the supernatant was saved and protein concentration was measured by BCA assay. Proteins (1 mg) were incubated with 20 μl of the immobilized phosphor-p38 (Thr180/Tyr182) antibody bead slurry overnight at 4°C. The immunoprecipitates were washed twice with lysis buffer and twice with kinase buffer. The pellets were then suspended in 50 μl of kinase buffer supplemented with 0.2 m*M* ATP and 1 μl ATF-2 for 30 min at 30°C. After incubation the kinase reaction was stopped by the addition of a 4×Laemmli sample buffer and 10 μl of the supernatant was subjected to SDS-PAGE. The band of phosphorylated ATF-2 was detected by a phospho-ATF-2 (Thr71) antibody.

Coimmunoprecipitation

Heart tissue samples were homogenized with ice-cold buffer (Tris 20 m*M*, pH 7.4, NaCl 150 m*M*, EDTA 1 m*M*, 0.5% Triton, and DTT 1 m*M*) supplemented with a cocktail of protease inhibitors. After centrifugation at 21,000 *g* for 30 min at 4°C, the supernatant was saved and protein concentration was measured by BCA protein assay. Tissue homogenates (1 mg protein) were diluted with Co-IP buffer (Tris 20 m*M*, pH 7.4, NaCl 150 m*M*, EGTA 10 m*M*, NaF 10 m*M*, and Triton 0.1%) and preincubated for 1 h with 20 μl protein A/G-agarose to remove any protein adhered nonspecifically to the beads. Then, 2 μg of anti-ASK1 antibody (Santa Cruz Biotechnology) was added to the precleared samples and incubated at 4°C overnight. After a second incubation with protein A/G agarose (25 μl at 4°C for 4 h, the immunocomplex was washed with Co-IP buffer. The pellet was boiled with 4×Laemmli sample buffer and separated by SDS-PAGE. The membrane was then probed with anti-Trx1 antibody (BD Pharmingen, Franklin Lakes, NJ).

TrxR assay

TrxR activity was measured by a method that employed a rapid procedure of direct DTNB reduction in the presence and in the absence of specific TrxR inhibitor to allow for correction of non-TrxR-dependent 5,5′-dithiobis(2-nitrobenzoic acid) (DTNB) reduction (37). Briefly, 200 μg of cytosolic protein was diluted with sample dilution buffer (potassium phosphate 100 m*M*, pH 7.0, and bovine serum albumin 2 mg/ml) to 120 μl and preincubated in the presence and in the absence of 100 n*M* auranofin (AF) for 10 min at room temperature. The reaction was started by the addition of 200 μl of assay mixture containing 100 m*M* potassium phosphate, pH 7.0, 10 m*M* EDTA, 0.24 m*M* NADPH, and 2.5 m*M* DTNB. The change in optical density was measured over a 5 min period at 412 nm using the kinetics program of a microplate spectrophotometer (Tecan, Research Triangle Park, NC). Data collection started 1 min after the initiation of the reaction to allow nonenzymatic reaction of DTNB to go to completion. TrxR activity was reported as nmol DTNB reduced per mg protein per min using an extinction coefficient of 13.6 ml/μmol.

Electrophysiological techniques

Aliquots of isolated myocytes were transferred to a cell chamber on the stage of an inverted microscope and superfused with a solution containing (in m*M*) 138 NaCl, 4.0 KCl, 1.2 $MgCl_2$, 1.8 $CaCl_2$, 18 glucose, 5 HEPES, and 0.5 $CdCl_2$ (to block Ca^{2+} channels), pH 7.4. Ionic currents were then recorded using the whole-cell configuration of the patch-clamp technique. Briefly, borosilicate glass capillaries were pulled (Sutter Instruments, Novato, CA) to an internal tip diameter of 1–2 μm, and filled with a pipette solution containing (in m*M*) 135 KCl, 3 $MgCl_2$, 10 HEPES, 3 Na_2-ATP, 10 EGTA, and 0.5 Na-GTP, pH 7.2. Filled pipettes with a resistance of 2–4 MΩ were coupled to a patch-clamp amplifier (Molecular Devices, Sunnyvale, CA). After correction of the liquid junction potential and creation of a GΩ seal, the membrane within the pipette was ruptured and at least 5 min was allowed for the contents of the pipette and cytoplasm to equilibrate. A computer program (Molecular Devices) controlled command potentials and acquired current signals that were filtered at 2 kHz. Currents were sampled at 4 kHz by a 12-bit resolution analog-to-digital converter and stored on the hard disk of a computer. All electrophysiological experiments were done at room temperature (22°C–24°C).

The I_{to} was evoked by 500 ms depolarizing pulses to test potentials between −40 and +60 mV (0.2 Hz). The holding potential was set at −80 mV and a 100 ms prepulse was applied to −60 mV to inactivate the fast Na^+ current. For each test pulse, I_{to} amplitude was measured as the difference between the peak outward current and the steady-state current level at the end of the depolarizing pulse. All electrophysiological data were normalized as current densities by dividing measured current amplitude (pA) by whole-cell capacitance (pF).

Statistical analysis

All results are expressed as mean ± standard error. Statistical comparisons of two groups were made using a Student's *t*-test, whereas comparisons of more than two groups were made by analysis of variance. When a significant difference between groups was indicated by the initial analysis, individual paired comparisons were made using a Student-Newman-Keuls *t*-test. Differences were considered significant at $p < 0.05$.

Results

JNK-p38 activation in post-MI heart

Disease-related oxidative stress in many cell types elicits activation of a network of kinases that signal compensatory

responses, including JNK and p38 (10–12, 19). Thus, the activity profiles of these stress-activated kinases were first examined in MI hearts by analyzing their phosphorylation status in tissue samples from surviving regions of the left ventricle and septum. Figure 1A shows representative examples of immunoblots demonstrating a marked increase in phosphorylated JNK (p-JNK) and p38 (p-p38) in MI hearts ($n = 6$) compared with sham controls ($n = 6$). In parallel experiments, kinase activities were determined by measuring the degree of phosphorylation of recombinant c-Jun, a JNK substrate, or ATF-2, a p38 substrate. As shown in Figure 1B and C, both JNK and p38 activities were significantly increased post-MI by twofold to eightfold over sham hearts, which is in agreement with increased phosphorylation of these kinases.

To assess the electrophysiological impact of JNK/p38 activation post-MI, voltage-clamp experiments were conducted in isolated ventricular myocytes to assess the magnitude of I_{to} density in response to kinase inhibitors. This K^+ current is downregulated in several disease states affecting the heart (2) and is perhaps the most consistent change observed in the electrically remodeled ventricle, including the human heart (14). Figure 2A shows superimposed raw current traces from an untreated post-MI myocyte and another treated with the JNK inhibitor SP600125 (10 μM) for 4–5 h, illustrating that JNK blockade markedly increased the magnitude of I_{to} density. Mean data from several myocytes are summarized in Figure 2B, which shows that SP600125 (filled squares) significantly increased I_{to} at test potentials from +10 to +60 mV. Indeed, maximum I_{to} density (+60 mV) in SP600125-treated myocytes from MI hearts (32.1 ± 4.5 pA/pF; $n = 8$) was not statistically different from sham controls (28.3 ± 2.0 pA/pF; $n = 15$). By comparison, treatment of myocytes from sham hearts with SP600125 had no significant effect on maximum I_{to} density (27.9 ± 3.6 pA/pF; $n = 10$) relative to untreated sham controls. A similar upregulation of I_{to} in MI myocytes was observed with a membrane-permeable peptide inhibitor, JNKI-1 (10 μM; filled triangles), whereas a negative control peptide (JNKI-Neg) had no effect. Since p38 kinase was also increased in MI hearts, we tested the electrophysiological effects of p38 inhibitors. Figure 2C shows that 4–5 h incubation of post-MI myocytes with one of two structurally distinct p38 inhibitors, SB203580 (10 μM) or PD169316 (10 μM), significantly increased maximum I_{to} density compared with untreated MI myocytes. As with JNK inhibition, SB203580 did not significantly alter I_{to} density in sham myocytes (31.0 ± 4.8 pA/pF; $n = 8$) compared with untreated controls. Finally, although p38 inhibitors clearly de-remodeled I_{to} in post-MI myocytes, the ERK inhibitor PD98059 (10 μM) had no effect on I_{to} density.

We have previously shown that activators of receptor tyrosine kinase signaling normalize I_{to} density in myocytes from diabetic rats (20) similar to JNK and p38 inhibitors in MI hearts. Thus, we examined the electrophysiological role of insulin-like growth factor-1 (IGF-1) in the present study since this growth factor has been shown to exert significant antioxidant and antiapoptotic effects on the myocardium (18, 36, 39, 44). As shown in Figure 3A, 10 nM IGF-1 for 4–5 h upregulated I_{to} density in myocytes from MI hearts (filled squares) to a similar extent as JNK/p38 inhibitors. Moreover, in a separate series of experiments this effect was blocked by the TrxR inhibitor AF (10 nM; filled diamonds), implicating the involvement of the Trx system in the regulation of Kv channels (22). In contrast to the response of post-MI myocytes, IGF-1 had no effect on I_{to} in

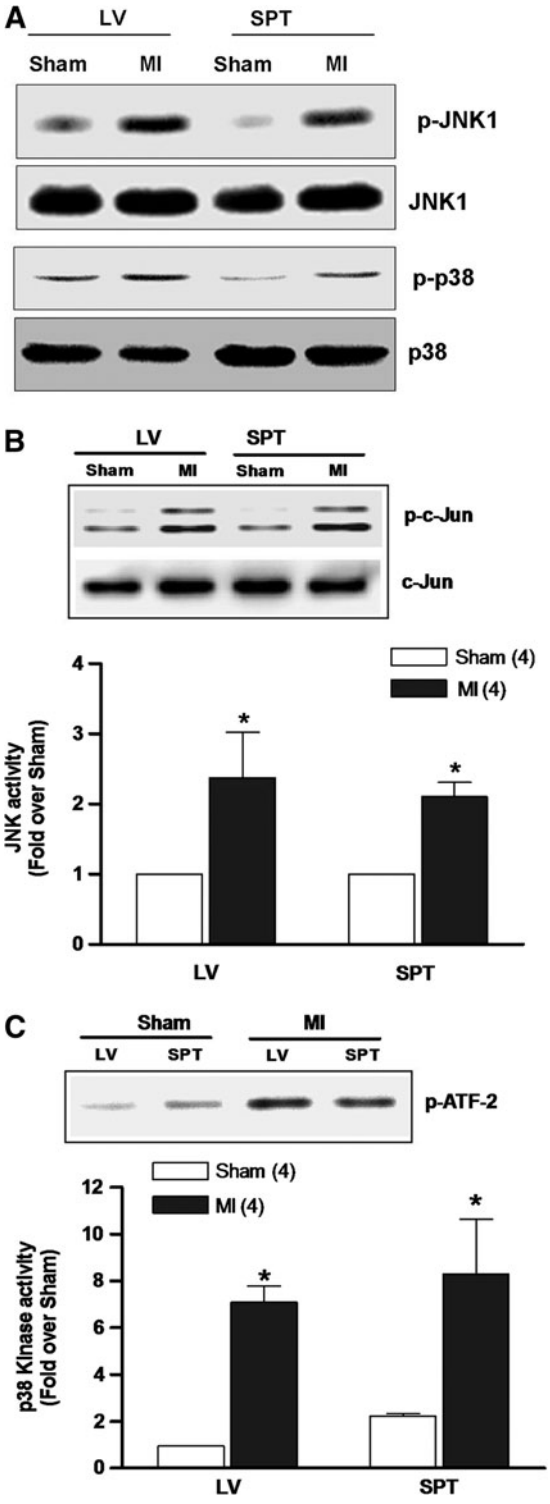

FIG. 1. JNK and p38 activity post-MI. (**A**) Representative immunoblots from six experiments of sham-operated and MI hearts using anti-p-JNK and anti-p-p38 antibody. The same blot was stripped and re-probed with anti-JNK and anti-p38 antibody to show total JNK and p38. (**B, C**) Comparisons of JNK and p38 kinase activity in post-MI and sham hearts. The *in vitro* kinase assay measured the phosphorylation of recombinant c-Jun (JNK substrate) or ATF-2 (p38 substrate). The relative kinase activity was determined by densitometry. *$p < 0.05$ compared with sham. LV, left ventricle; SPT, septum; JNK, c-Jun NH_2-terminal kinase; MI, myocardial infarction.

myocytes from sham rats (Fig. 3B). It should also be noted that an insulin-mimetic exhibited similar effects as IGF-1, further supporting the link between receptor tyrosine kinase signaling and Kv channel activity. Specifically, the compound *bis*-peroxovanadium-1,10-phenanthroline [bpV(phen); 10 μM], which acts as an insulin mimetic by inhibiting protein tyrosine phosphatase (32), increased maximum I_{to} density in post-MI myocytes after 4–5 h (26.7 ± 5.7 pA/pF; $n = 9$) similar to IGF-1 (32.7 ± 2.9 pA/pF; $n = 17$), but had no significant effect on myocytes from sham hearts (26.4 ± 3.3 pA/pF; $n = 6$). However, despite I_{to} upregulation by IGF-1 and bpV(phen), 100 nM insulin did not affect I_{to} density in myocytes from MI hearts (15.1 ± 1.9 pA/pF; $n = 8$), suggesting that the ventricular dysfunction elicited by MI is accompanied by insulin resistance (27).

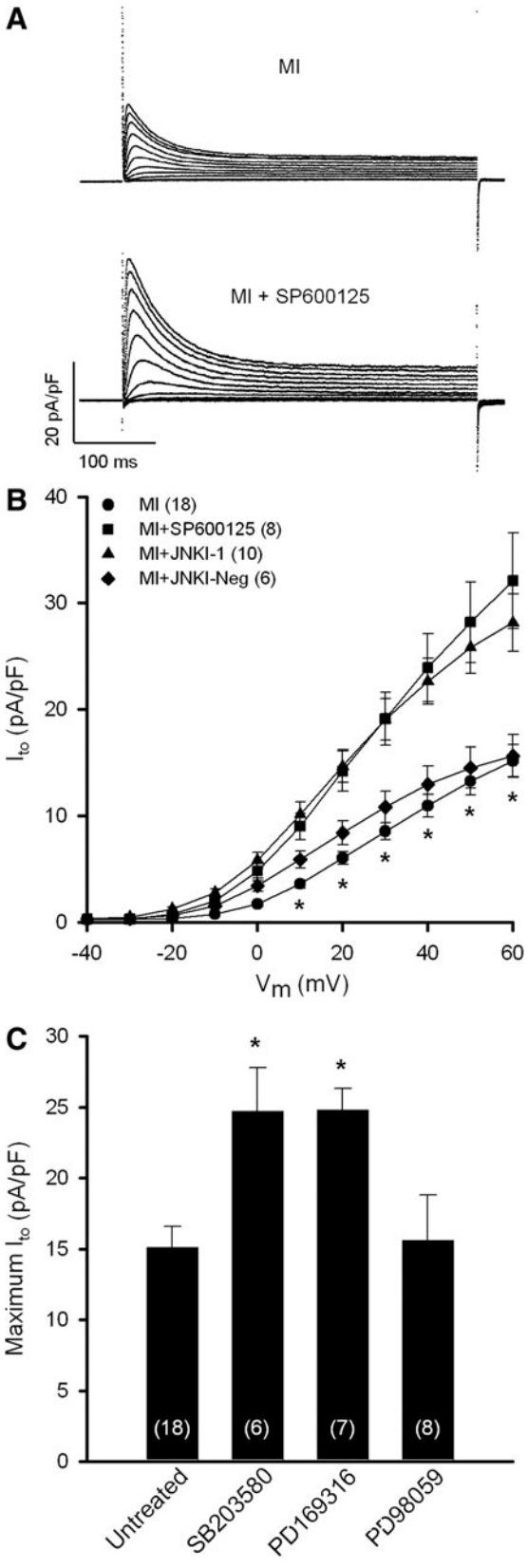

FIG. 2. Upregulation of I_{to} density by JNK and p38 inhibitors. (**A**) Superimposed current traces are shown for myocytes from post-MI hearts untreated or treated with the JNK inhibitor SP600125 (10 (μM) for 4–5 h. (**B**) Mean I-V relations of I_{to} illustrate de-remodeling effect of SP600125 or inhibitory peptide JNKI-1 (10 (μM). JNKI-Neg, negative control peptide for JNKI-1. *$p < 0.05$ compared with SP600125- and JNKI-1-treated myocytes. (**C**) De-remodeling of I_{to} by p38 inhibition with SB203580 or PD169316 (10 (μM). *$p < 0.05$ compared with untreated MI group. I_{to}, transient outward K^+ current. Numbers in parentheses represent number of myocytes sampled.

IGF-1-mediated regulation of ASK1-JNK-p38 signaling

Given that JNK/p38 inhibitors and IGF-1 upregulated the density of I_{to} in myocytes from MI hearts, we tested the hypothesis that the electrophysiological effects of IGF-1 were mediated by a decrease in JNK/p38 activity. Specifically, experiments were done in isolated heart preparations perfused through the coronary vasculature with oxygenated culture medium at 37°C *via* the Langendorff method. Figure 4A shows that in MI hearts perfused with 10 nM IGF-1 for 4–5 h, phosphorylation levels of JNK (p-JNK) and p38 (p-p38) measured by Western blot were decreased compared with hearts that were not treated and that this effect was blocked by 10 nM AF. In parallel kinase assay experiments summarized in Figure 4B and C, the marked increases in JNK and p38 activities observed in MI hearts relative to shams were significantly attenuated by IGF-1, which was blocked by pretreatment with AF. We also explored a major upstream regulator of JNK/p38, ASK1, and its association with its endogenous inhibitor Trx1. In these studies, cell lysates from excised tissue samples were first treated with ASK1 antibody and the immunoprecipitate used in Western blots performed with Trx1 antibody. These coimmunoprecipitation assays, which are illustrated in Figure 5A, showed that ASK1–Trx1 interaction was decreased in MI hearts, consistent with activation of ASK1-JNK-p38 signaling. To determine whether IGF-1 affected ASK1-Trx1 binding, additional organ culture experiments were done in sham and MI hearts perfused with IGF-1. In the MI hearts IGF-1 significantly increased the density of ASK1-Trx1 bands, suggesting increased binding, and this effect was blocked by AF. However, sham hearts treated with IGF-1 for 4–5 h showed decreased ASK1-Trx1 binding similar to that observed in untreated MI hearts, even though IGF-1 had no significant effect on I_{to} density in sham myocytes (Fig. 3B). This suggests that IGF-1 may acutely activate ASK1-JNK-p38 signaling in sham hearts. Thus, to explore this possibility we examined the phosphorylation levels of JNK and p38 by Western blot in IGF-1-treated sham hearts and, as

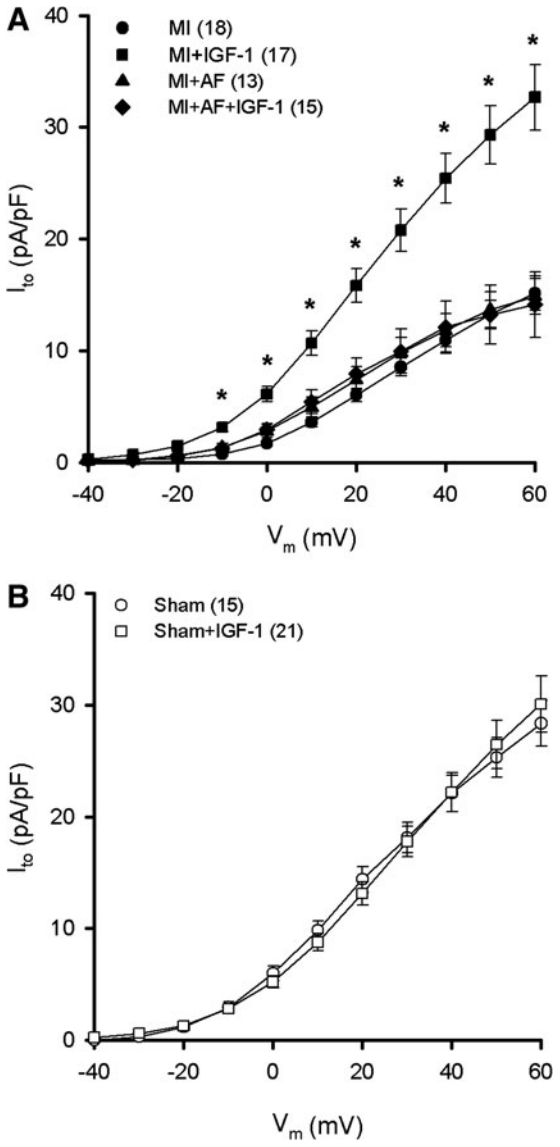

FIG. 3. Upregulation of I_{to} density by IGF-1. (**A**) Myocytes from MI hearts were treated with 10 n*M* IGF-1 for 4–5 h in the presence or absence of the TrxR inhibitor AF (10 n*M*). *$p < 0.05$ compared with untreated MI group (filled circles). (**B**) Myocytes from sham hearts treated with IGF-1 for 4–5 h. AF, auranofin; IGF-1, insulin-like growth factor-1; TrxR, thioredoxin reductase.

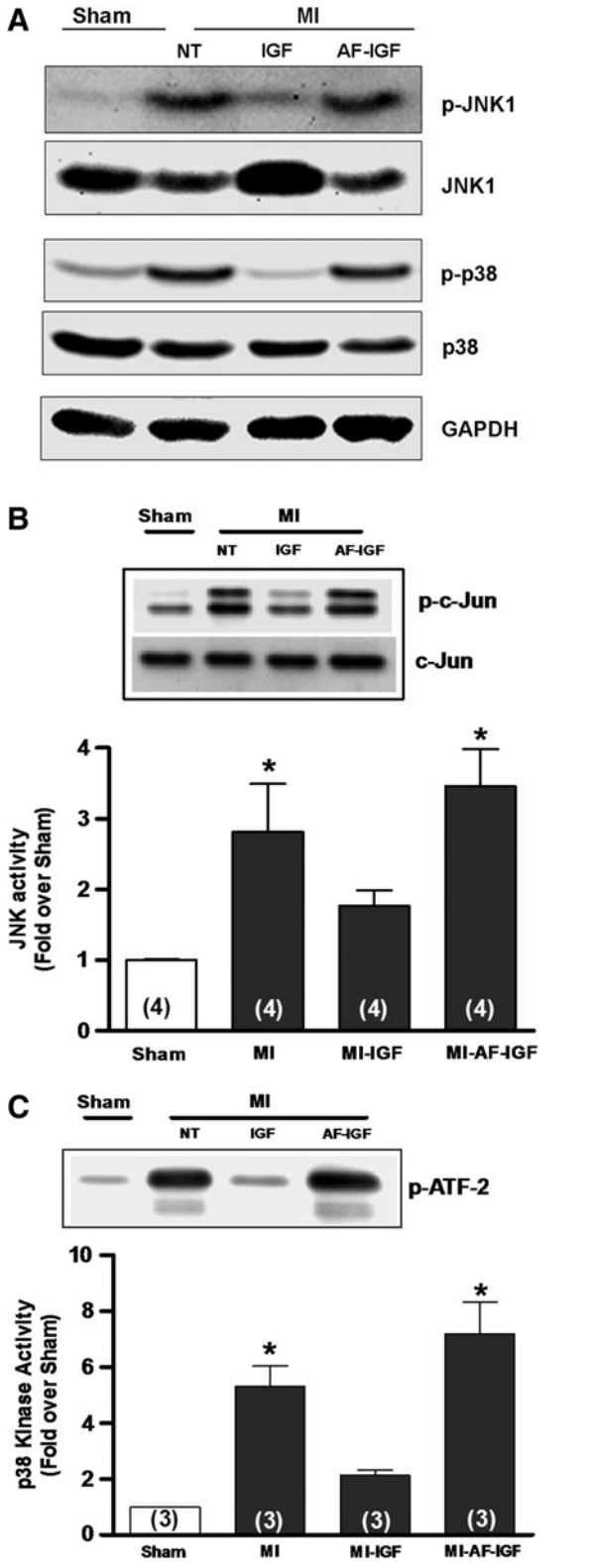

FIG. 4. Attenuation of JNK and p38 activity by IGF-1. (**A**) Representative Western blot of p-JNK/JNK and p-p38/p38. The same blot was stripped and re-probed with GAPDH to show equal loading. (**B**) JNK activity assay. (**C**) p38 kinase activity assay. The relative kinase activity was determined by densitometry. *$p < 0.05$ compared with sham. GAPDH, glyceraldehyde 3-phosphate dehydrogenase. Numbers in parentheses in this and subsequent figures represent number of hearts sampled.

shown in Figure 5C, found significant increases compared with untreated sham hearts. These data thus highlight marked differences in IGF-1 signaling in MI and sham hearts and the electrophysiological effects of ASK1-JNK-p38 activation.

The lack of response of MI preparations to IGF-1 in the presence of AF (Figs. 3A, 4B, 4C, and 5B) supports the involvement of the Trx system in regulating Kv channel expression, as we have proposed previously (20, 22). Thus, to explore the relationship of IGF-1 signaling with the Trx system, protein expression and activity of TrxR1 were examined in tissue samples from perfused heart preparations. Figure 6 shows that protein abundance (panel A) and activity (panel B) of TrxR1 in the left ventricle were significantly decreased in MI hearts compared with shams (22) and that this difference was atten-

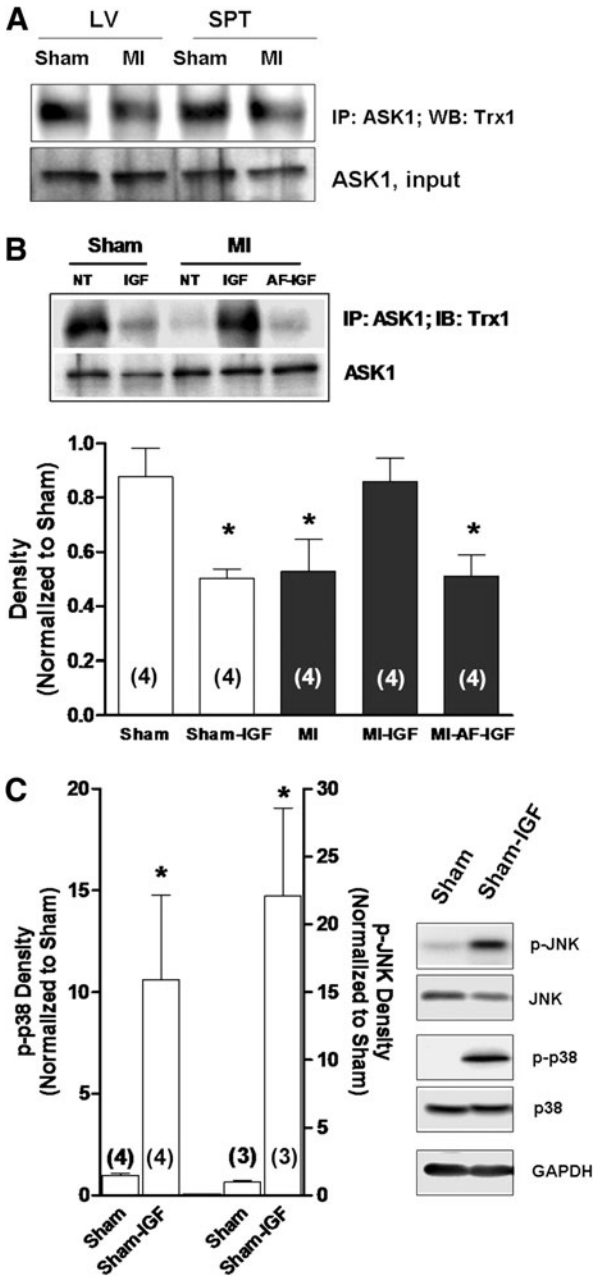

FIG. 5. Inhibition of ASK1 activation by Trx1. (**A**) Representative blot of four experiments from Trx1-ASK1 co-immunoprecipitation. Trx1 binding was decreased in MI heart, which indirectly indicates activation of ASK1. The blot was stripped and re-probed with ASK1 antibody to show equal loading. (**B**) Role of TrxR in IGF-1-mediated recovery of Trx1-ASK1 binding in MI hearts. ASK1-Trx1 interaction was assessed by densitometry. (**C**) Phosphorylation levels of p38 and JNK determined by Western blot in sham hearts perfused with IGF-1. Representative blots are shown to the right. $^*p < 0.05$ compared with untreated sham group. ASK1, apoptosis signal-regulating kinase-1.

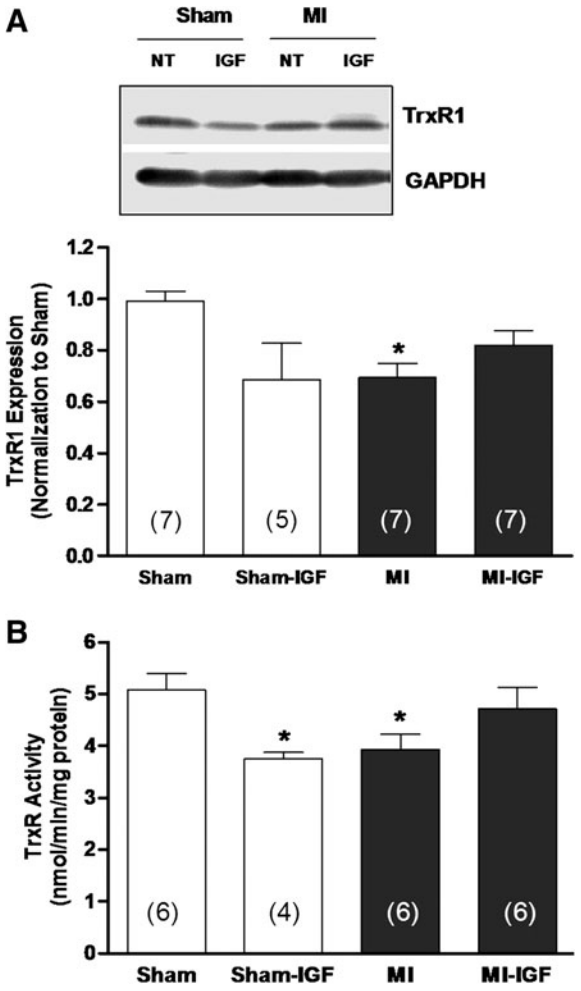

FIG. 6. Protein expression and activity of TrxR1. (**A**) Western blot analysis of TrxR1 protein abundance in sham-operated and MI hearts perused with IGF-1 for 4–5 h. $^*p < 0.05$ compared with untreated sham. (**B**) TrxR1 activity measured by direct DTNB reduction in sham and MI hearts perused for 4–5 h with IGF-1. Assays were performed in the presence and absence of AF to allow for correction of non-TrxR-dependent DTNB reduction. $^*p < 0.05$ compared with untreated sham.

uated after treating MI hearts with IGF-1 for 4–5 h. In contrast to these data, IGF-1 decreased TrxR1 protein and activity in sham hearts although the decrease in protein abundance did not reach significance. Moreover, since IGF-1 significantly increased I_{to} density in post-MI myocytes (Fig. 3A), we examined the protein abundance of the major α-subunit that carries this current, Kv4.2. Figure 7A shows that in untreated hearts perfused for 4–5 h, the protein abundance of Kv4.2 was significantly less in the MI group compared with sham controls (open bar), as shown previously (22). However, MI hearts perfused with IGF-1 showed a marked increase in Kv4.2 protein expression, although not to the level of sham hearts. Nevertheless, these findings agree with the upregulation of I_{to} density observed in isolated MI myocytes (Fig. 3A). Also in agreement with our electrophysiological data (Fig. 3B), IGF-1 had no significant effect on Kv4.2 protein levels in sham hearts (Fig. 7B).

Discussion

Stress-activated kinases and Kv channels

Oxidative stress is postulated to play a prominent role in the etiology of ventricular dysfunction associated with

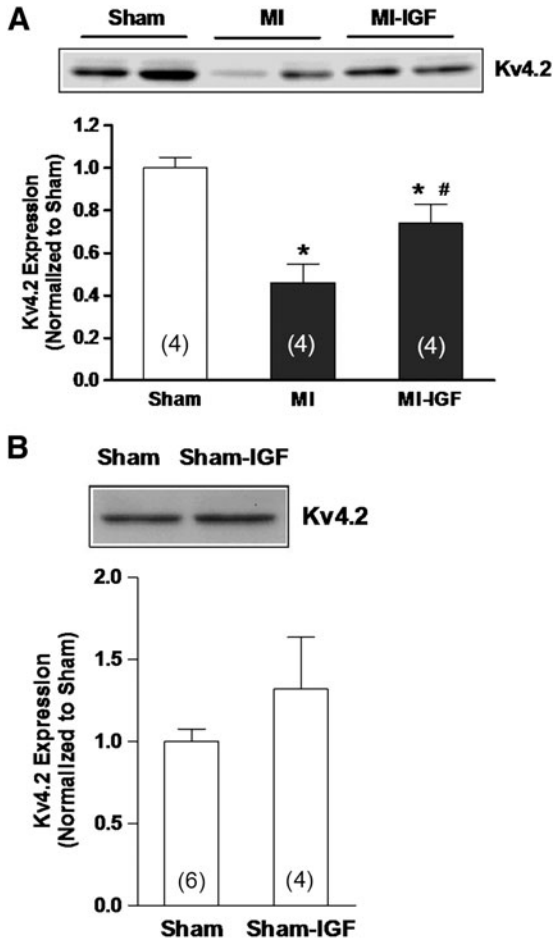

FIG. 7. Upregulation of Kv4.2 protein by IGF-1. (**A**) Membrane proteins of sham-operated, untreated, and IGF-1-treated MI hearts were subject to sodium dodecyl sulfate-polyacrylamide gel electrophoresis. Kv4.2 protein expression was determined by densitometry. $^{*}p < 0.05$ compared with sham. $^{\#}p < 0.05$ compared with untreated MI. (**B**) Kv4.2 protein abundance in sham hearts treated with IGF-1.

cardiovascular disease (12, 19, 26, 30, 35, 45). The biological impact of excess reactive oxygen species (ROS) levels on cardiac myocytes involves changes in the redox state of proteins, some of which can be reversed. In part, reversible protein oxidation involves the free thiol (-SH) side chain of cysteine residues that can undergo a number of ROS-mediated molecular modifications that may elicit positive or negative changes in protein function (5, 30, 38, 45). The redox status of protein thiols is controlled largely by disulfide oxidoreductase networks such as the Trx and Grx systems, which function to maintain thiols in their normally reduced state and to detoxify ROS (5, 30). Moreover, the redox-active effectors of these systems, namely, reduced Trx and Grx, also regulate intracellular signaling molecules and transcription factors by direct binding (29, 38, 45). Thus, under conditions where ROS levels are markedly elevated and/or oxidoreductase systems are impaired, there is significant alteration in physiological function of cells mediated by direct protein oxidation or changes in protein interaction with redox molecules.

Stress-activated protein kinases such as JNK and p38 are ROS-sensitive regulators of cardiac hypertrophy and apoptosis in response to disease conditions (10–12, 18, 19, 24). In the heart damaged by ischemia-reperfusion or chronic MI, JNK and p38 are stimulated (Fig. 1) and their activities can be decreased by antioxidant therapies (19). Our present data also implicate these kinases as contributing to the remodeling of ventricular Kv channels. Specifically, inhibitors of JNK or p38 upregulated I_{to} density in myocytes from MI hearts after several hours of treatment (Fig. 2), but the targets of these kinases that mediate changes in the electrophysiological phenotype have not yet been identified. Moreover, it is presently unclear why both types of inhibitors had essentially the same positive effect. This finding may reflect cross-talk between JNK and p38 pathways (31) or co-operative action at a common downstream target such as a transcription factor or an accessory regulator of channel expression (43).

The etiology of decompensated heart failure involves a constellation of changes in myocardial structure, metabolism, and electrophysiology, a process termed remodeling. Our laboratory and others have shown that downregulation of Kv currents, particularly I_{to}, is a hallmark of ventricular electrical remodeling that develops in different disease states (2, 15, 20, 22, 33). Recently, we have identified oxidative stress and impaired oxidoreductase activity as key contributors to the downregulation of Kv4 channel expression and I_{to} density in failing rat heart (20, 22, 33). In particular, we have shown that the Trx system is mainly involved in regulating Kv4 channels and I_{to} density during the remodeling elicited by type 1 diabetes (20) or chronic MI (22). In both cases the Trx system is significantly impaired, as evidenced by decreased TrxR1 mRNA, protein abundance, and activity (22). Although the targets of the Trx system involved in disease-induced changes in Kv channel expression are largely unknown, our present data suggest that binding of Trx1 with ASK1 may be involved (see below).

De-remodeling of Kv channels by IGF-1 in post-MI hearts

While decreased I_{to} density is a hallmark of the electrically remodeled ventricle, we have demonstrated in experimental disease states of diabetes (20) and chronic MI (22, 33) that this phenotype is reversible, a process termed de-remodeling. In the diabetic heart, de-remodeling of I_{to} is stimulated *in vitro* by insulin and is prevented by TrxR inhibitors (20). In the post-MI heart, we found that IGF-1 similarly de-remodeled I_{to} in a TrxR-dependent manner (Fig. 3A). These findings suggest that the Trx system in the MI and diabetic heart is stimulated by receptor tyrosine kinase signaling, and our current data further imply that this stimulation is at the level of TrxR since IGF-1 increased its protein abundance and activity (Fig. 6). Although not specifically examined in the present study, increased reducing activity by the Trx system is also likely from metabolic effects of IGF-1 mediated by increased glucose uptake (3, 36) and possibly increased NADPH production by the pentose phosphate pathway (3). Thus, we propose that the salient redox effect of IGF-1 on myocytes from MI hearts was an increase in the amount a reduced Trx secondary to increased TrxR activity and supply of NADPH, which promoted the *de novo* synthesis of Kv4.2 protein (Fig. 7A) and possibly accessory subunits (22). However, it is also possible that post-translational modifications of Kv4.2 protein thiols were elicited by the Trx system, since the increase in I_{to}

density by IGF-1 in post-MI myocytes was nearly twice that of the increase in Kv4.2 protein abundance. Indeed, we and others have shown evidence of post-translational redox regulation of Kv4 channels (23, 41).

Our current data also suggest that a key redox-sensitive factor participating in I_{to} remodeling during chronic MI is ASK1, a mitogen-activated protein kinase kinase that activates JNK and p38 (12, 13, 29). ASK1 is uniquely regulated by oxidative stress through direct binding with reduced Trx1, which inhibits kinase activity (12, 25, 29, 38, 45). In some cell types reduced Grx1 has also been shown to bind and inhibit ASK1 (38). It is proposed that in the presence of ROS, Trx1 is oxidized, which releases ASK1, enabling it to phosphorylate JNK and p38 (12). However, dissociation of Trx1 from ASK1 alone may not be sufficient to activate JNK, which may further require oxidation of a specific cysteine residue (Cys250) on ASK1 (28). Nevertheless, our findings suggest that ASK1-mediated activation of JNK and p38 in post-MI hearts participates in downregulating Kv channel expression. In support of this hypothesis, we found that binding of Trx1 with ASK1 was decreased in the MI heart (Fig. 5), implying that ASK1 was activated, and that upon treatment with IGF-1 Trx1-ASK1 binding was restored to control (sham) levels in a TrxR-dependent manner (Fig. 5B). However, our experiments cannot rule out participation of other mechanisms that have been shown to regulate ASK1 activity. For example, redox-sensitive Ca^{2+}-calmodulin kinase II and the Ca^{2+}-regulated phosphatase calcineurin activate ASK1 *via* phosphorylation (16, 24). On the other hand, the serine/threonine kinase Akt, which is activated by IGF-1, has been shown to inhibit ASK1, thus supporting a pro-survival role (1, 7, 17). We also cannot rule out ASK1-independent regulation of JNK and p38, such as by activation of specific isoforms of protein kinase C (9). Hence, the role played by ASK1 in downregulating Kv channels in the failing heart and the specific redox mechanisms involved have yet to be fully defined.

IGF-1 effects in sham hearts

Although our data point to the ASK1-JNK-p38 pathway as participating in Kv channel remodeling during chronic cardiac dysfunction, the response of sham hearts to IGF-1 indicates that there are marked differences in signaling between pathological and physiological states of the myocardium. Specifically, IGF-1 elicited acute changes in ASK1-Trx1 binding, JNK/p38 phosphorylation, and TrxR1 expression in sham hearts that were similar to untreated MI hearts (Figs. 5 and 6), yet expression of Kv4.2 protein was not altered by IGF-1 in the sham group (Fig. 7B). Moreover, when myocytes from sham hearts were treated with IGF-1 I_{to} density did not change, unlike the significant upregulation in post-MI myocytes (Fig. 3). It is possible that the lack of Kv channel remodeling in sham hearts by IGF-1 is related to unique cellular responses to acute *versus* sustained activation of ASK1-JNK-p38 signaling (12, 18, 39, 40). It is also possible that distinct isoforms of JNK or p38 (26, 31, 34) are involved in Kv channel downregulation that are activated by pathogenic (*e.g.*, angiotensin II and endothelin) but not physiologic (*e.g.*, IGF-1) stimuli. Finally, specific interactions of activated JNK/p38 with scaffold proteins that regulate signaling specificity, integration, and subcellular localization (6, 10, 43) may differ between normal and disease states of the heart, which may control whether or not Kv channel expression is decreased.

As with ASK1-JNK-p38 signaling, the effects of IGF-1 on TrxR1 expression and activity were opposite in MI and sham hearts (Fig. 6), and thus the precise relationship between the Trx system and Kv4 channel expression is unclear. We reported previously that short-term (4–6 h) treatment of isolated ventricular myocytes from sham hearts with AF did not significantly decrease I_{to} density (46), but in another study we showed that normal rats treated for 3 days with buthionine sulfoximine (a blocker of GSH synthesis) plus 1,3-*bis*-(2-chloroethyl)-1-nitrosourea (an inhibitor of TrxR and glutathione reductase) had marked decreases in Kv4 channel mRNA, protein abundance, and I_{to} density in the LV (21). In agreement with the present study, downregulation of I_{to} density with oxidoreductase inhibition was also reversed *in vitro* by stimulation of receptor tyrosine kinase signaling with the insulin-mimetic, bpV(phen) (21). Thus it would appear that long-term inhibition of TrxR is linked to Kv4 channel downregulation, but the involvement of JNK or p38 in this pharmacological model was not examined. Nevertheless, it is clear that the relationship of cell redox state, oxidoreductase networks, and ASK1-JNK-p38 signaling in diseased and normal hearts remains to be clarified.

In summary, our data suggest that expression of cardiac Kv channels is redox regulated and that chronic impairment of the Trx system in the heart with MI contributes to I_{to} remodeling through sustained activation of ASK1-JNK-p38 signaling. Stimulation of receptor tyrosine kinase signaling in the MI heart by IGF-1 inhibits ASK1-JNK-p38 activity and upregulates Kv4 channels in a TrxR-dependent manner, but this response is in contrast to sham hearts where IGF-1 acutely activates ASK1-JNK-p38 but has no effect on Kv4 channel expression or I_{to} density. We postulate therefore that the Trx system may be a novel therapeutic target to prevent arrhythmias in the electrically remodeled and failing heart.

Acknowledgment

This work was supported by National Heart, Lung and Blood Institute Grant, HL-66446 (to G.J. Rozanski).

Author Disclosure Statement

No competing financial interests exist.

References

1. Aikin R, Maysinger D, and Rosenberg L. Cross-talk between phosphatidylinositol 3-kinase/AKT and c-Jun NH_2-terminal kinase mediates survival of isolated human islets. *Endocrinology* 145: 4522–4531, 2004.
2. Armoundas AA, Wu R, Juang G, Marban E, and Tomaselli GF. Electrical and structural remodeling of the failing ventricle. *Pharmacol Ther* 92: 213–230, 2001.
3. Dimitriadis G, Parry-Billings M, Dunger D, Bevan S, Colquhoun A, Taylor A, Calder P, Krause U, Wegener G, and Newsholme EA. Effects of *in-vivo* administration of insulin-like growth factor-1 on the rate of glucose utilization in the soleus muscle of the rat. *J Endocrinol* 133: 37–43, 1992.
4. Fedorov VV, Lozinsky IT, Sosunov EA, Anyukhovsky EP, Rosen MR, Balke CW, and Efimov IR. Application of blebbistatin

as an excitation-contraction uncoupler for electrophysiologic study of rat and rabbit hearts. *Heart Rhythm* 4: 619–626, 2007.
5. Fernandes AP and Holmgren A. Glutaredoxins: glutathione-dependent redox enzymes with functions far beyond a simple thioredoxin backup system. *Antioxid Redox Signal* 6: 63–74, 2004.
6. Finn SG, Dickens M, and Fuller SJ. C-Jun N-terminal kinase-interacting protein 1 inhibits gene expression in response to hypertrophic agonists in neonatal rat ventricular myocytes. *Biochem J* 358: 489–495, 2001.
7. Galvan V, Logvinova A, Sperandio S, Ichijo H, and Bredesen DE. Type 1 insulin-like growth factor receptor (IGF-IR) signaling inhibits apoptosis signal-regulating kinase 1 (ASK1). *J Biol Chem* 278: 13325–13332, 2003.
8. Greenstein JL, Wu R, Po S, Tomaselli GF, and Winslow RL. Role of the calcium- independent transient outward current I_{to1} in shaping action potential morphology and duration. *Circ Res* 87: 1026–1033, 2000.
9. Hausenloy DJ and Yellon DM. Survival kinases in ischemic preconditioning and postconditioning. *Cardiovasc Res* 70: 240–253, 2006.
10. He H, Li HL, Lin A, and Gottlieb RA. Activation of the JNK pathway is important for cardiomyocyte death in response to simulated ischemia. *Cell Death Differ* 6: 987–991, 1999.
11. Honsho S, Nishikawa S, Amano K, Zen K, Adachi Y, Kishita E, Matsui A, Katsume A, Yamaguchi S, Nishikawa K, Isoda K, Riches DWH, Matoba S, Okigaki M, and Matsubara H. Pressure-mediated hypertrophy and mechanical stretch induces IL-1 release and subsequent IGF-1 generation to maintain compensative hypertrophy after affecting Akt and JNK pathways. *Circ Res* 105: 1149–1158, 2009.
12. Hori M and Nishida K. Oxidative stress and left ventricular remodeling after myocardial infarction. *Cardiovasc Res* 81: 457–464, 2009.
13. Izumiya Y, Kim S, Izumi Y, Yoshida K, Yoshiyama M, Matsuzawa A, Ichijo H, and Iwao H. Apoptosis signal-regulating kinase 1 plays a pivotal role in angiotensin II-induced cardiac hypertrophy and remodeling. *Circ Res* 93: 874–883, 2003.
14. Kääb S, Dixon J, Duc J, Ashen D, Nabauer M, Beuckelmann DJ, Steinbeck G, McKinnon D, and Tomaselli GF. Molecular basis of transient outward potassium current downregulation in human heart failure. A decrease in Kv4.3 mRNA correlates with a reduction in current density. *Circulation* 98: 1383–1393, 1998.
15. Kaprielian R, Wickenden AD, Kassiri Z, Parker TG, Liu PP, and Backx PH. Relationship between K^+ channel downregulation and $[Ca^{2+}]_I$ in rat ventricular myocytes following myocardial infarction. *J Physiol* 517(Pt 1): 229–245, 1999.
16. Kashiwase K, Higuchi Y, Hirotani S, Yamaguchi O, Hikoso S, Takeda T, Watanabe T, Taniike M, Nakai A, Tsujimoto I, Matsumura Y, Ueno H, Nishida K, Hori M, and Otsu K. CaMKII activates ASK1 and NF-κB to induce cardiomyocyte hypertrophy. *Biochem Biophys Res Commun* 327: 136–142, 2005.
17. Kim A, Khursigara G, Sun X, Franke TF, and Chao MV. Akt phosphorylates and negatively regulates apoptosis signal-regulating kinase 1. *Mol Cell Biol* 21: 893–901, 2001.
18. Krause D, Lyons A, Fennelly C, and O'Connor R. Transient activation of Jun N-terminal kinases and protection from apoptosis by the insulin-like growth factor 1 receptor can be suppressed by dicumarol. *J Biol Chem* 276: 19244–19252, 2001.
19. Li WG, Coppey L, Weiss RM, and Oskarsson HJ. Antioxidant therapy attenuates JNK activation and apoptosis in the remote noninfarcted myocardium after large myocardial infarction. *Biochem Biophys Res Commun* 280: 353–357, 2001.
20. Li X, Li S, and Rozanski GJ. Redox regulation of K^+ channel remodeling in diabetic rat heart. *Am J Physiol Heart Circ Physiol* 288: H1417–H1424, 2005.
21. Li X, Li S, Xu Z, Lou MF, Anding P, Liu D, Roy SK, and Rozanski GJ. Redox control of K^+ channel remodeling in rat ventricle. *J Mol Cell Cardiol* 40: 339–349, 2006.
22. Li X, Tang K, Xie B, Li S, and Rozanski GJ. Regulation of Kv4 channel expression in failing rat heart by the thioredoxin system. *Am J Physiol Heart Circ Physiol* 295: H416–H424, 2008.
23. Liang H, Li X, Li S, Zheng MQ, and Rozanski GJ. Oxidoreductase regulation of Kv currents in rat ventricle. *J Mol Cell Cardiol* 44: 1062–1071, 2008.
24. Liu Q, Sargent MA, York AJ, and Molkentin JD. ASK1 regulates cardiomyocyte death but not hypertrophy in transgenic mice. *Circ Res* 105: 1110–1117, 2009.
25. Liu Y and Min W. Thioredoxin promotes ASK1 ubiquitination and degradation to inhibit ASK1-mediated apoptosis in a redox activity-independent manner. *Circ Res* 90: 1259–1266, 2002.
26. Mukherjee S, Lekli I, Das M, Azzi A, and Das DK. Cardioprotection with α-tocopheryl phosphate: amelioration of myocardial ischemia reperfusion injury is linked with its ability to generate a survival signal through Akt activation. *Biochim Biophys Acta* 1728: 498–503, 2008.
27. Murray AJ, Lygate CA, Cole MA, Carr CA, Radda GK, Neubauer S, and Clarke K. Insulin resistance, abnormal energy metabolism and increased ischemic damage in the chronically infracted rat heart. *Cardiovasc Res* 71: 149–157, 2006.
28. Nadeau PJ, Charette SJ, and Landry J. Redox reaction at ASK1-Cys250 is essential for activation of JNK and induction of apoptosis. *Mol Biol Cell* 20: 3628–3637, 2009.
29. Nishida K and Otsu K. The role of apoptosis signal-regulating kinase 1 in cardiomyocyte apoptosis. *Antioxid Redox Signal* 8: 1729–1736, 2006.
30. Nordberg J and Arner ES. Reactive oxygen species, antioxidants, and the mammalian thioredoxin system. *Free Radic Biol Med* 31: 1287–1312, 2001.
31. Perdiguero E, Ruiz-Bonilla V, Serrano AL, and Muñoz-Cánoves P. Genetic deficiency of p38α reveals its critical role in myoblast cell cycle exit. The p38α-JNK connection. *Cell Cycle* 6: 1298–1303, 2007.
32. Posner BJ, Faure R, Burgess JW, Bevan AP, Lachance D, Zhang-Sun G, Fantus IG, Ng JB, Hall DA, Lum BS, and Shaver A. Peroxovanadium compounds. A new class of potent phosphotyrosine phosphatase inhibitors which are insulin mimetics. *J Biol Chem* 296: 4596–4604, 1994.
33. Rozanski GJ and Xu Z. Glutathione and K^+ channel remodeling in postinfarction rat heart. *Am J Physiol Heart Circ Physiol* 282: H2346–H2355, 2002.
34. Saurin AT, Martin JL, Heads RJ, Foley C, Mockridge JW, Wright MJ, Wang Y, and Marber MS. The role of differential activation of p38-mitogen-activated protein kinase in preconditioned ventricular myocytes. *FASEB J* 14: 2237–2246, 2000.
35. Seddon M, Looi YH, and Shah AM. Oxidative stress and redox signaling in cardiac hypertrophy and heart failure. *Heart* 93: 903–907, 2007.

36. Singleton JR and Feldman EL. Insulin-like growth factor-1 in muscle metabolism and myotherapies. *Neurobiol Dis* 8: 541–554, 2001.
37. Smith AD and Levander OA. High-throughput 96-well microplate assay for determining specific activities of glutathione reductase and thioredoxin reductase. *Methods Enzymol* 347: 113–121, 2002.
38. Song JJ and Lee YJ. Differential role of glutaredoxin and thioredoxin in metabolic oxidative stress-induced activation of apoptosis signal-regulating kinase1. *Biochem J* 373: 845–853, 2003.
39. Teos LY, Zhao A, Alvin Z, Laurence GG, Li C, and Hadda GE. Basal and IGF-1-dependent regulation of potassium channels by MAP kinases and PI3-kinase during eccentric hypertrophy. *Am J Physiol Heart Circ Physiol* 295: H1834–H1845, 2008.
40. Tobiume K, Matsuzawa A, Takahashi T, Nishitoh H, Morita K, Takeda K, Monowa O, Miyazono K, Noda T, and Ichijo H. ASK1 is required for sustained activations of JNK/p38 MAP kinases and apoptosis. *EMBO Rep* 2: 222–228, 2001.
41. Wang G, Strang C, Pfaffinger PJ, and Covarrubias M. Zn^{2+}-dependent redox switch in the intracellular T1-T1 interface of a Kv channel. *J Biol Chem* 282: 13637–13647, 2007.
42. Wang WZ, Gao L, Wang HJ, Zucker IH, and Wang W. Interaction between cardiac sympathetic afferent reflex and chemoreflex is mediated by the NTS AT1 receptors in heart failure. *Am J Physiol Heart Circ Physiol* 295: H1216–H1226, 2008.
43. Whitmarsh AJ. The JIP family of MAPK scaffold proteins. *Biochem Soc Trans* 34: 828–832, 2001.
44. Yamamura T, Otani H, Nakao Y, Hattori R, Osako M, and Imamura H. IGF-1 differentially regulates Bcl-xL and Bax and confers myocardial protection in the rat heart. *Am J Physiol Heart Circ Physiol* 280: H1191–H1200, 2001.
45. Zhang H, Tao L, Jiao X, Gao E, Lopez BL, Christopher TA, Koch W, and Ma XL. Nitrative thioredoxin inactivation as a cause of enhanced myocardial ischemia/reperfusion injury in the aging heart. *Free Radic Biol Med* 43: 39–47, 2007.
46. Zheng MQ, Tang K, Zimmerman MC, Liu L, Xie B, and Rozanski GJ. Role of γ-glutamyl transpeptidase in redox regulation of K^+ channel remodeling in postmyocardial infarction rat hearts. *Am J Physiol Cell Physiol* 297: C253–C262, 2009.

Address correspondence to:
Dr. George J. Rozanski
Department of Cellular and Integrative Physiology
University of Nebraska Medical Center
985850 Nebraska Medical Center
Omaha, NE 68198-5850

E-mail: grozansk@unmc.edu

Date of first submission to ARS Central, January 13, 2010; date of final revised submission, May 26, 2010; date of acceptance, June 2, 2010.

Abbreviations Used

AF = auranofin
ASK1 = apoptosis signal-regulating kinase-1
BCA = bicinchoninic acid
bpV(phen) = *bis*-peroxovanadium-1,10-phenanthroline
DTNB = 5,5′-dithiobis(2-nitrobenzoic acid)
EGTA = ethylene glycol-bis(2 aminoethyl-ether)-*N*,*N*,*N*′,*N*′-tetraacetic acid
GAPDH = glyceraldehyde 3-phosphate dehydrogenase
Grx = glutaredoxin
IGF-1 = insulin-like growth factor-1
I_{to} = transient outward K^+ current
JNK = c-Jun NH_2-terminal kinase
Kv = voltage-gated K^+
MI = myocardial infarction
ROS = reactive oxygen species
SDS-PAGE = sodium dodecyl sulfate-polyacrylamide gel electrophoresis
TE = Tris-ethylenediaminetetraacetic acid
Trx = thioredoxin
TrxR = thioredoxin reductase